pubs.acs.org/acschemicalbiology

Article

Probing the Signal Transduction Mechanism of the Light-Activated Adenylate Cyclase OaPAC Using Unnatural Amino Acid Mutagenesis

Samruddhi S. Jewlikar, Jinnette Tolentino Collado, Madeeha I. Ali, Aya Sabbah, YongLe He, James N. Iuliano, Christopher R. Hall, Katrin Adamczyk, Gregory M. Greetham, Andras Lukacs,* Stephen R. Meech,* and Peter J. Tonge*

Cite This: https://doi.org/10.1021/acschembio.4c00627

Read Online

ACCESS | Metrics & More | Article Recommendations | Supporting Information

ABSTRACT: OaPAC, the photoactivated adenylyl cyclase from *Oscillatoria acuminata*, is composed of a blue light using FAD (BLUF) domain fused to an adenylate cyclase (AC) domain. Since both the BLUF and AC domains are part of the same protein, OaPAC is a model for understanding how the ultrafast modulation of the chromophore binding pocket caused by photoexcitation results in the activation of the output domain on the μs-s time scale. In the present work, we use unnatural amino acid mutagenesis to identify specific sites in the protein that are involved in transducing the signal from the FAD binding site to the ATP binding site. To provide insight into site-specific structural dynamics, we replaced W90 which is close to the chromophore pocket, F103 which interacts with W90 across the dimer interface, and F180 in the central core of the AC domain, with the infrared probe azido-Phe (AzPhe). Using ultrafast IR, we show that AzPhe at position 90 responds on multiple time scales following photoexcitation. In contrast, the light minus dark IR spectrum of AzPhe103 shows only a minor perturbation in environment between the dark and light states, while replacement of F180 with AzPhe resulted in a protein with no catalytic activity. We also replaced Y125, which hydrogen bonds with N256 across the dimer interface, with fluoro-Tyr residues. All the fluoro-Tyr substituted proteins retained the light-induced red shift in the flavin absorption spectrum; however, only the 3-FY125 OaPAC retained photoinduced catalytic activity. The loss of activity in 3,5-F_2Y125 and 2,3,5-F_3Y125 OaPAC, which potentially increase the acidity of the Y125 phenol by more than 1000-fold, suggests that deprotonation of Y125 disrupts the signal transduction pathway from the BLUF to the AC domain.

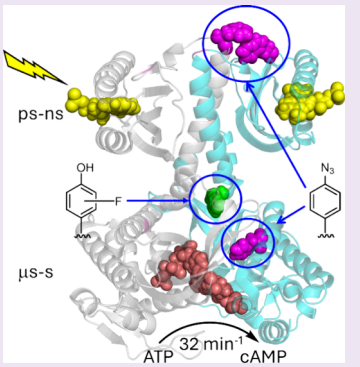

INTRODUCTION

Optogenetics combines optical and genetic approaches to control cellular events using light.[1] Central to this technology are photoactive proteins that are fused to effector domains to enable light-dependent control of processes such as enzyme activity, gene expression, and signaling. The rational design and optimization of new optogenetic devices require a detailed understanding of the photoactivation mechanism of naturally occurring photoreceptors, particularly those in which both the light absorbing and effector domains are part of the same protein. Flavin-dependent photoreceptors, including those that contain blue light using FAD (BLUF) or light oxygen voltage (LOV) domains, are popular choices for the creation of novel optogenetic tools,[2,3] and a key goal is to determine how ultrafast excitation of the flavin chromophore results in formation of the light-activated state on the μs-s time scale.[4,5]

BLUF domain photoreceptors are found in bacteria and unicellular eukaryotes,[6] where light-activated signaling is accomplished through either noncovalent or covalent interaction with downstream effector output partners. BLUF photoreceptors control a diverse array of physiological processes including photosystem biogenesis (AppA),[7] phototaxis (PixD/Slr1694),[8] and virulence (BlsA).[9] In addition, BLUF domain photoreceptors have been discovered that regulate the production of the important signaling molecule cAMP in response to blue light, including PACα and PACβ from *Euglena gracilis*,[10] bPAC from *Beggiatoa*,[11] and OaPAC from *Oscillatoria acuminata*.[12]

OaPAC is a 366 residue homodimer containing an N-terminal BLUF domain and a C-terminal class III adenylate cyclase (AC) domain (Figure 1).[12] The two monomers interact in a head to head configuration, with each BLUF domain providing a helix to a coiled coil that connects the BLUF domain with the AC domain. Similar to other BLUF photoreceptors, the BLUF domain is comprised of a ferredoxin-like fold in which the isoalloxazine ring of the flavin is surrounded by two α-helices and a five-stranded β-sheet.[13−16] In addition, several conserved residues form a hydrogen bond network that interacts with the isoalloxazine

Received: September 17, 2024
Revised: January 10, 2025
Accepted: January 14, 2025

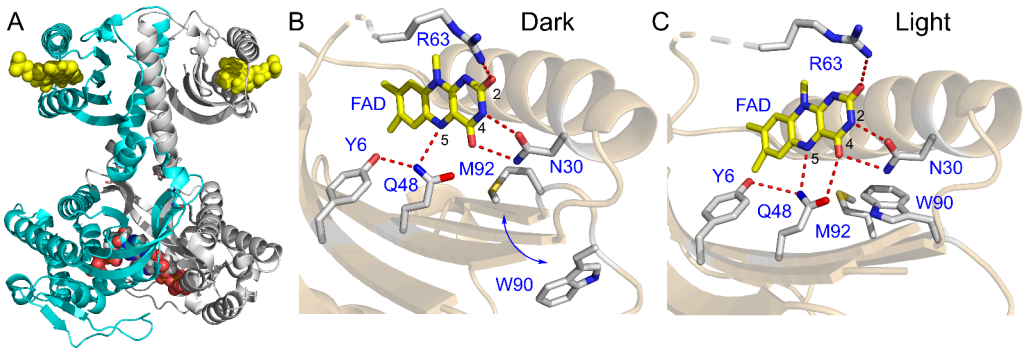

Figure 1. OaPAC dimer and flavin binding pocket. (A) OaPAC dimer (PDB: 8QFE). FAD and ATP are shown as spheres in the BLUF and AC domains, respectively. (B,C) Proposed structural changes in the flavin binding pocket upon photoactivation based on the structures of OaPAC determined by time-resolved crystallography (PDB: 8QFE and 8GFG).[26] Figure was made using pymol.[27]

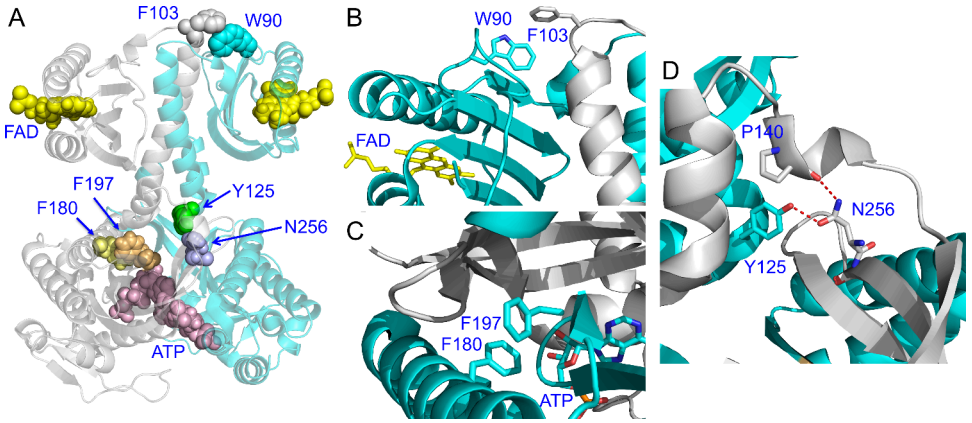

Figure 2. Residues replaced with unnatural amino acids. (A) OaPAC dimer depicting the residues chosen for substitution. (B) W90 and F103 were replaced with AzPhe. These residues interact across the dimer interface at the tip of the central helix. (C) F180 was replaced by AzPhe. (D) Y125 was replaced by fluoro-Tyr analogs. Figure was made using pymol,[27] from PDB: 8QFE.[26]

ring including Y6, Q48, and N30.[6,12] Light absorption results in an ∼10 nm red shift in the spectrum of the oxidized isoalloxazine chromophore which is caused by an increase in hydrogen bonding to the flavin C4═O group from the conserved Gln (Q48 in OaPAC).[17,18] Initial models for the change in hydrogen bonding involved rotation of the Gln side chain,[13,16] subsequently proposed to involve keto−enol tautomerism of the amide.[19,20] However, additional experimental and theoretical studies now support a mechanism that only involves tautomerization of the Gln amide side chain (Figure 1).[19,21−25]

While some of the light-stimulated changes in the BLUF photoreceptors are well understood, outstanding mechanistic issues include the role of electron transfer in photoactivation and the position of a semiconserved Trp (W90) and conserved Met (M92) which may communicate changes in the hydrogen bond network to the protein matrix.[28−31] Although radical intermediates are not observed in the photocycles of all BLUF proteins,[32,33] in OaPAC, the excitation of FAD leads to a concerted proton-coupled electron transfer (PCET) from Y6 to the oxidized flavin leading to the formation of the neutral flavin radical (FADH$^{\bullet}$). Subsequently, the Tyr-flavin radical pair recombines to form the final light state in which the flavin is again in the oxidized state.[34] In addition, the structural dynamics that drive output domain activation remain to be fully elucidated. To address one of these questions, we previously replaced Y6, the conserved Tyr in the OaPAC, with fluoro-Tyr residues to increase the acidity of the phenolic hydroxyl group. While the 3F−Y6 and 2,3-F_2Y6 variants underwent the complete photocycle and catalyzed the conversion of ATP into cAMP, the activity was abolished in the 3,5-F_2Y6 and 2,3,5-F_3Y6 variants where the photocycle was halted at FAD$^{\bullet-}$, demonstrating that proton transfer plays an essential role in initiating the structural reorganization of the AC domain.[34] We also previously studied the roles of conserved Gln, Q48, and D67 in photoactivation. These studies demonstrated that the Q48E mutation alters the primary electron transfer process and switches the enzyme to a permanently "on" state,[35] whereas replacing D67 with Asn accelerated the primary electron transfer process.[36] In the present work, we explore signal transduction at a more remote location from flavin by studying Y125.

Most BLUF proteins, including OaPAC, contain a Trp that is located near the flavin binding site (W90 in OaPAC). Structural studies of multiple BLUF proteins together with biophysical experiments and site-directed mutagenesis support a key role for Trp in photoactivation. In particular, it has been proposed that the indole side chain rotates between Trp_{in} and Trp_{out} conformations accompanied possibly by relocation of the conserved Met (M92 in OaPAC). Using cryo-trapping, Chretien et al. obtained support for this model and propose that W90 moves from a Trp_{out} to a Trp_{in} conformation during light state formation that is accompanied by the movement of M92 out of the pocket (Figure 1).[26] However, this model contrasts with earlier structural data on OaPAC in which the

https://doi.org/10.1021/acschembio.4c00627
ACS Chem. Biol. XXXX, XXX, XXX−XXX

Table 1. Absorbance Maxima and Catalytic Activity of the OaPAC Variants

OaPAC	dark λ_{max} (nm)	light λ_{max} (nm)	τ_{rec} [a] (s)	k_{cat} (min^{-1})	K_m (μM)	k_{cat}/K_m [b] (μM^{-1} min^{-1})
Wild-type	445	457	4	11.8 ± 1.1	65 ± 20	0.18 ± 0.05
F103AzPhe	444	455	4	8.8 ± 0.2	102 ± 7	0.09 ± 0.02
W90AzPhe	444	456	28	12.3 ± 0.4	103 ± 12	0.12 ± 0.03
F180AzPhe	444	456	5	NA[c]	NA[c]	NA[c]
3F−Y125	443	457	9	9.4 ± 1.4	86 ± 38	0.11 ± 0.04
3,5-F_2Y125	443	456	6	NA[c]	NA[c]	NA[c]
2,3,5-F_3Y125	444	454	4	NA[c]	NA[c]	NA[c]
N256A	444	457	7	NA[c]	NA[c]	NA[c]
N256Q	445	458	4	NA[c]	NA[c]	NA[c]
N256D	444	451	7	NA[c]	NA[c]	NA[c]

[a]Rate of dark state recovery was monitored at 443 nm. [b]Catalytic activity was determined by quantifying the rate of PPi formation following irradiation. at 450 nm. Errors are the standard deviation from two or more biological replicates. [c]NA, no detectable activity.

Trp undergoes only a relatively small movement and is found in a Trp_{out} conformation in both dark and light states.[12,37]

Photoexcitation of OaPAC results in an ∼100-fold increase in the synthesis of cAMP from ATP, indicating that adenylate cyclase activity is efficiently suppressed in the dark state.[34] To provide further details on the mechanism of photoactivation, we employed site-directed and unnatural amino acid mutagenesis coupled with time-resolved and steady-state FT-IR spectroscopy as well as kinetic assays to probe the local structural changes in OaPAC and map the signal transduction pathway in solution. Following similar studies on the BLUF proteins AppA and PixD,[38] we replaced W90 with the infrared (IR) probe azido-Phe (AzPhe). We also introduced AzPhe into two other positions in the OaPAC at F103 and F180. F103 is on a loop between β-sheet 5 and α-helix 3, which undergoes a significant structural rearrangement on photoactivation,[26] whereas F180 is in the central core of the AC domain (Figure 2). Finally, we analyzed the importance of Y125, which is located at the junction between the α-3 helix and the AC domain and interacts across the dimer interface with N256, by replacing this residue with fluoro-Tyr residues. Key findings based on the spectroscopic and kinetic characterization of the substituted OaPAC proteins include support for the movement of W90 from a Trp_{out} to a Trp_{in} conformation during light state formation and that signal transduction requires Y125 to be protonated. Collectively, the data provide further insight into the mechanism of signal transduction in OaPAC.

RESULTS

AzPhe as an IR Probe of Local Structural Dynamics.

AzPhe has previously been used to explore the structural changes experienced by specific residues in the BLUF proteins AppA and PixD caused by photoactivation[38] and in other photoreceptors such as Channelrhodopsin[39] and bacteriophytochrome.[40] To extend these studies to the present system, we identified three positions in the OaPAC based on their location in the protein: W90 which is proposed to play a pivotal role in photoactivation, F103 which is present on the loop between β-sheet 5 and α-helix 3 and interacts with the "out" conformation of W90 across the dimer interface, and F180 which is in the core of the AC domain.

W90AzPhe, F103AzPhe, and F180AzPhe OaPAC were expressed using 21st pair methodology,[41] using an OaPAC construct with a C-terminal His-tag. Following purification with Ni-affinity chromatography, the UV−visible absorption spectrum and rate of dark state recovery were determined for each protein (Figures S1 and S2). Similar to wild-type OaPAC, each AzPhe-substituted protein underwent the characteristic red shift in the flavin absorption spectrum and recovered to the dark state with $\tau \sim 5$ s with the exception of W90AzPhe which recovered ∼5-fold more slowly ($\tau \sim 28$s) (Table 1).

The dark and light state activities of each protein were assessed using a discontinuous assay that monitored the time-dependent formation of inorganic pyrophosphate (PPi) (Table 1, Figure S3). Whereas W90AzPhe and F103AzPhe had activity in the light state similar to the wild-type enzyme, F180AzPhe OaPAC had no detectable activity (Table 1).

We then obtained light minus dark steady state FTIR spectra of W90AzPhe, F103AzPhe, and F180AzPhe on an OaPAC (Figure 3). The azido stretching vibration of W90AzPhe

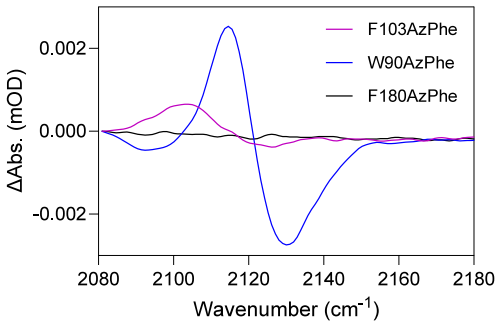

Figure 3. Difference infrared spectra of the AzPhe OaPAC variants. Light minus dark steady-state infrared spectra of W90AzPhe (blue), F103AzPhe (purple), and F180AzPhe (black). Difference spectra were acquired by subtracting the FTIR spectrum of the sample obtained before irradiation from that obtained during continuous 450 nm irradiation.

demonstrated a significant perturbation between the light and dark states, whereas only a minor perturbation was observed for F103AzPhe, revealing that the environment of the AzPhe residue at position 103 is similar in the two states of the protein. In addition, no change was observed in the environment of F180AzPhe, consistent with the observation that this mutation leads to a catalytically inactive enzyme. The experiment was repeated multiple times on each sample allowing the photoreceptor to recover to the dark state before subsequent irradiation. Comparison of the azido mode after three cycles of irradiation and recovery revealed no change in the infrared intensity, indicating that the wavelength of light used did not cause any unwanted photochemistry of the azido group (Figure S4).

https://doi.org/10.1021/acschembio.4c00627
ACS Chem. Biol. XXXX, XXX, XXX−XXX

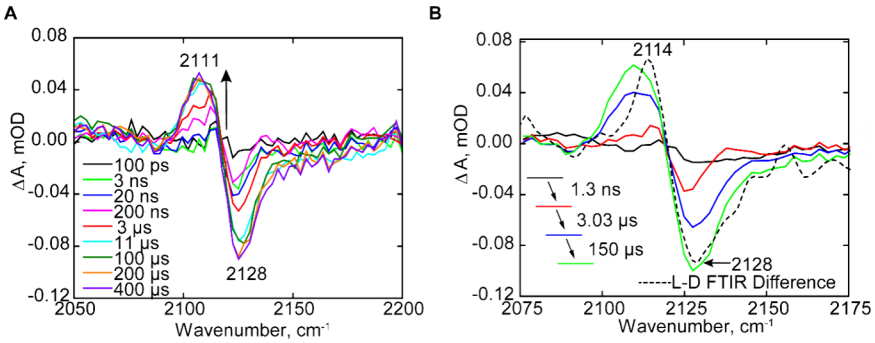

Figure 4. TRMPS spectra of the W90AzPhe OaPAC dark state. (A) Time-resolved IR difference response of the azido mode following ultrafast excitation of isoalloxazine cofactor in OaPAC at the W90 position. (B) EADS of W90AzPhe obtained from globally fitting the time-resolved data in A to a sequential first order kinetics model with an initial state (black) and two intermediate states (red, blue), which form on a ns-μs time scale and subsequently relaxes to a final state (green). Final state is compared with the FTIR difference spectra (black dash line). All analyses used the Glotaran software package.

To provide further information about the environmental changes experienced by W90AzPhe, we used ultrafast IR to monitor the difference spectrum of the azido stretch as a function of time following light absorption (Figure 4). The temporal evolution of the AzPhe at W90 position shows a negative bleach at 2128 cm^{-1} within ~1 ns and deepens on the μs time scale as a transient at 2111 cm^{-1} evolves. Figure 4B shows the evolution-associated difference spectra (EADS), which represent the spectral evolution over time. To generate the EADS, time-resolved data (Figure 4A) were globally analyzed in Glotaran using a sequential decay model of four components in which the lifetime of three components was allowed to vary, while the fourth component was kept constant (indicating a product with effectively infinite lifetime), yielding three time constants of 1.3, 3.03, and 150 μs. The final spectrum of the W90AzPhe evolves on the μs time scale and is similar to the steady-state IR difference spectrum. Unlike the TRIR of W104AzPhe $AppA_{BLUF}$ and W91AzPhe PixD,[38] no evolution of the IR spectrum of W90AzPhe OaPAC is detected on the ps time scale. The instantaneous response of the W104AzPhe in AppA and W91AzPhe in PixD was taken as evidence for communication of the AzPhe with the hydrogen bond network surrounding the flavin, i.e., a Trp_{in} conformation, and the absence of an instantaneous perturbation in the spectrum of W90AzPhe is thus consistent with a Trp_{out} conformation in OaPAC.

We also measured the time-resolved IR spectra of W90AzPhe OaPAC in the fingerprint region to correlate the protein structural changes with the dynamics observed in the azido region (Figure 5). The EADS, generated by a global fit of

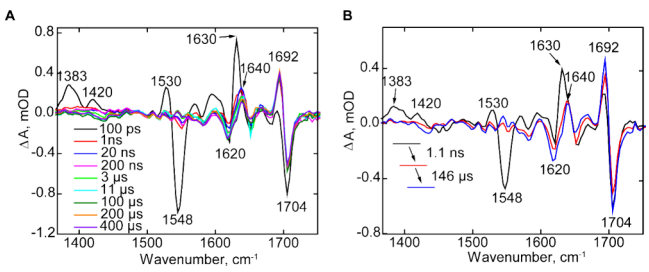

Figure 5. TRMPS of the W90AzPhe OaPAC dark state. (A) Temporal evolution of the W90AzPhe OaPAC spectra recorded between 100 fs and 1 ms after 450 nm excitation. (B) EADS of W90AzPhe OaPAC obtained from a global fit of the data in (A).

the data using two time constants of 1.1 ns and 146 μs, shows that key intermediate states form within the first 3 ns that are detected in both the fingerprint and azido stretch regions of the spectrum and likely represent changes to the chromophore and proximal protein matrix. Comparison to the data obtained for wild-type OaPAC[34] indicates that the AzPhe substitution has not affected the overall photocycle. For instance, the 1530 cm^{-1} indicates the formation of $FADH^{\bullet}$, and thus, PCET has not been affected, while the 1692 (+)/1704 (−) cm^{-1} transient can be assigned to a red shift of the flavin C4═O mode due to the additional hydrogen bond formed between the C4═O and Q48 in the light state of OaPAC. The subsequent slower changes on the μs time scale, such as the transients at 1640 (+)/1620 (−) cm^{-1} assigned to protein secondary structure, correlate with the evolution of the AzPhe and result from the formation of the final signaling state of the protein.

Intersubunit Hydrogen Bond between Y125 and N256. Y125 is a fully conserved residue across all photoactivated adenylate cyclase enzymes and is present at the interface between the α3 helix and the AC domain, where it forms an intersubunit hydrogen bond with N256. Replacement of Y125 with Phe results in a catalytically inactive protein,[12] a result also observed in the related photoreceptor bPAC.[42] We prepared the Y125F mutant and confirmed by size-exclusion chromatography that the mutation did not affect the oligomerization state of the protein (Figure S5). To provide more information on the role of this key hydrogen bonding interaction in transducing the signal from the BLUF to the AC domain, we modulated the acidity of the Y125 hydroxyl group by replacing Y125 (pK_a 9.9) with 3-fluoro-Tyr (3-FY, pK_a 8.4), 3,5-difluoro-Tyr (3,5-F_2Y, pK_a 7.2), and 2,3,5-trifluoro-Tyr (2,3,5-F_3Y, pK_a 6.4). We also replaced N256 with Ala, Asp, and Gln residues.

The fluoro-Tyr variants were prepared, as described in the methods section, and the UV−visible absorption spectrum and rate of dark state recovery were determined for each protein (Figures S1 and S2). As observed for the AzPhe variants, the 443 nm FAD absorption band for each fluoro-Tyr protein red-shifted by ~12 nm upon illumination and recovered to the dark state with τ ~ 4−9 s (Table 1). We then analyzed the catalytic activity of each variant and found that the 3F−Y125 OaPAC retained light-activated adenylate cyclase activity (Figure S3), while replacing Y125 with 3,5-difluoro-Tyr and 2,3,5-trifluoro-Tyr resulted in a loss of activity in the light state.

https://doi.org/10.1021/acschembio.4c00627
ACS Chem. Biol. XXXX, XXX, XXX−XXX

Michaelis−Menten parameters for the 3F−Y125 OaPAC were similar to those for the wild-type enzyme (Table 1).

Given the effect of lowering the Y125 pK_a on catalytic activity, we attempted to determine the pH dependence of the wild-type enzyme. However, whereas OaPAC had similar activity at pH 8−9, no activity was observed at pH 7.0 and 7.5, preventing the pH dependence from being determined (Figure S6). The loss of activity resulting from a relatively small change in pH may reflect a pH-induced structural change of the protein rather than the change in the ionization state of a single residue. We also replaced N256 with Ala, Asp, and Gln residues. Although each N256 mutant retained the light-induced red shift in FAD absorbance that recovered to the dark state on a similar time scale to that of wild-type OaPAC (τ 4−7 s), none of these OaPAC mutants had detectable catalytic activity (Table 1), again supporting the importance of the Y125−N256 hydrogen bond in the formation of the OaPAC light state.

DISCUSSION

OaPAC complex is a light-activated adenylate cyclase in which both the photosensing and catalytic domains are part of the same protein. As a consequence, OaPAC is a model for elucidating the mechanism of signal transduction in BLUF photoreceptors, information that is critical to the design and optimization of novel optogenetic devices. In the present work, we have used unnatural amino acid mutagenesis to evaluate key sites thought to be critical for photoactivation including W90 which lies close to the chromophore, F103 which is present on the loop between β-sheet 5 and α-helix 3 and interacts with W90 across the dimer interface, F180 which is in the adenylate cyclase domain, and Y125 which forms an intersubunit hydrogen bond with N256 in the OaPAC dimer.

The IR probe AzPhe was used to replace W90, F103, and F180. All three OaPAC variants retained the characteristic red shift in FAD absorbance upon illumination and recovered to the dark state with similar rates as the wild type, although W90AzPhe OaPAC recovered ∼5-fold more slowly (Table 1). It was subsequently found that F180AzPhe was catalytically inactive, and in keeping with this observation, the steady-state light minus dark FTIR difference spectra of AzPhe180 OaPAC indicated that there was no change in the environment of the AzPhe group upon photoexcitation (Figure 3). Therefore, the F180AzPhe mutation prevents the activation of the adenylate cyclase domain and is locked in the dark state, although the protein environment around flavin responds to light absorption. Analysis of the X-ray structure of OaPAC shows that F180 forms a $\boldsymbol{\pi-\pi}$ stacking interaction with F197, and previous studies have shown that the F197S mutation is catalytically inactive supporting the functional importance of the F180−F197 interaction.[12]

In contrast to F180AzPhe OaPAC, both the W90AzPhe and F103AzPhe OaPAC variants had similar catalytic activity in the light state compared to wild-type OaPAC (Table 1). FTIR difference spectra of these variants indicated a red shift in the azido mode upon photoexcitation; however, the intensity of the difference spectrum for F103AzPhe OaPAC is significantly smaller than that for W90AzPhe OaPAC. F103 is located on the loop between β-sheet 5 and α-helix 3 which undergoes a significant structural rearrangement on photoactivation.[26] However, the low intensity of the F103AzPhe IR difference spectrum suggests that the AzPhe group experiences a similar environment in both the dark and lights states. Thus, either the azido group in F103AzPhe does not interact with W90 in the dark state or W90 occupies similar positions in the dark and light states.

Many BLUF domain photoreceptors contain a Trp that is located close to the flavin binding pocket, including the OaPAC (W90). This includes the BLUF proteins AppA and PixD (Srl1694) where structural data revealed that the conserved Trp (W104 in AppA and W91 in PixD) can adopt a conformation in which the indole side chain is close to the flavin binding pocket (Trp_{in}) or has rotated out of the pocket (Trp_{out}).[13,16,43] Replacement of W104 with Ala in AppA decouples the light-induced changes in the flavin binding pocket from protein structural changes, and this observation together with other structural, biochemical, biophysical, and computational studies indicates that the Trp is directly involved in signal transduction, leading to the proposal that movement of the Trp is linked to the formation of the light-activated state.[19,44−47] A Met residue is also located close to the Trp (M106 in AppA and M93 in PixD), resulting in proposed models in which the Trp and Met side chains exchange positions during photoactivation. To determine the dynamics of the Trp and Met residues in AppA and PixD, we replaced each residue with AzPhe and used TRIR to analyze the time-dependent evolution of the azido IR spectrum. Although AzPhe substituted for M106 and M93 responded only weakly to excitation, the azido spectrum of AzPhe at positions 104 and 91 responded instantaneously and then showed complex evolution on the sub-ns time scale leading to the conclusion that the AzPhe occupies an "in" configuration, in both $AppA_{BLUF}$ and PixD, consistent with solution NMR studies.[15,48]

Site-directed mutagenesis also supports a critical mechanistic role for W90 in OaPAC,[49] and X-ray structural studies have shown that W90 occupies a Trp_{out} conformation in the dark state.[12,26,37] Although the initial "light state" structure of OaPAC showed only a small perturbation in the position of W90,[12,37] the recent time-resolved X-ray structural studies on OaPAC provide support for the movement of W90 from a Trp_{out} to a Trp_{in} conformation and relocation of M92 away from the flavin.[26] In addition, ^{19}F NMR experiments suggest that W90 can occupy multiple positions ($W_{in}NH_{in}$, $W_{in}NH_{out}$, and W_{out}) and that the prevalence of Trp_{out} conformations observed in the X-ray structures of BLUF proteins may be the result of crystal packing.[48] Thus, to provide further insight into the structural dynamics of W90, we used TRIR in addition to steady-state FTIR to analyze time-dependent changes in the IR spectrum of W90AzPhe OaPAC. Both the W90AzPhe azido stretch at ∼2100 cm^{-1} and the fingerprint region respond on similar time constants to photoexcitation (1.3 ns, 3.03, and 150 μs compared to 1.1 and 140 μs), indicating that incorporation of AzPhe has not decoupled excitation of the flavin from activation of the adenylate cyclase domain, in agreement with the enzyme activity data. However, unlike the TRIR data for W104AzPhe $AppA_{BLUF}$ and W91AzPhe PixD, the AzPhe in OaPAC does not respond instantaneously to excitation, consistent with a Trp_{out} conformation in the dark state of OaPAC in contrast to the Trp_{in} conformation for $AppA_{BLUF}$ and PixD. The subsequent evolution of W90AzPhe on slower time scales reflects the protein structural changes that lead to the light-activated state of OaPAC in which the AzPhe now samples a different environment consistent with a Trp_{in} conformation.

https://doi.org/10.1021/acschembio.4c00627
ACS Chem. Biol. XXXX, XXX, XXX−XXX

We also studied the importance of hydrogen bonding interactions between Y125 and N256 at the OaPAC dimer interface. Previous studies had shown that Y125F was catalytically inactive,[37,42] and we also demonstrated that replacement of N256 with Ala, Gln, or Asp resulted in loss of activity. We then modulated the pK_a of Y125 by replacing this residue with fluoro-Tyr analogues that vary the acidity of the Tyr hydroxyl group. While 3F-Y125 OaPAC had activity similar to that of wild-type OaPAC, neither the 3,5-F_2Y125 nor 2,3,5F_3Y125 OaPAC variants had detectable activity in the dark and light states. One possible explanation for this result is that Y125 has to be protonated for signal transduction to occur and that in 3,5-F_2Y125 and 2,3,5-F_3Y125 OaPAC, the Tyr is deprotonated. To test this hypothesis, we attempted to protonate the fluoro-Tyr residues by lowering the pH. However, control experiments with wild-type OaPAC indicated that the enzyme rapidly lost activity at pH values below 8. All of the fluoro-Tyr and N256 variants retained the red shift in the FAD absorbance and recovered to the dark state at rates similar to that of wild-type OaPAC, indicating that light-induced changes in the chromophore binding pocket are decoupled from enzyme activation.

MATERIALS AND METHODS

Materials. 3-Fluorophenol, 2,6-difluorophenol, FAD, pyridoxal phosphate, and L-azido-Phe (AzPhe) were purchased from Sigma-Aldrich. 2,3,6-Trifluorophenol was purchased from Oakwood Chemical. The E3 orthogonal polyspecific aminoacyl-tRNA synthetase used to incorporate the fluoro-Tyr analogues and the pDule aminoacyl-tRNA synthetase (pDule-pCNPhe) used to incorporate AzPhe were generous gifts from Professor Joanne Stubbe, MIT, and Professor Ryan Mehl, Oregon State University, respectively.[50,51]

Tyrosine Phenol Lyase Expression and Purification. BL21-(DE3) pLysS cells were transformed with the pET23b C-terminal His-TPL plasmid, and a single colony was used to inoculate 10 mL of LB media supplemented with 100 μg/mL ampicillin (Amp) and 30 μg/mL chloramphenicol (Cam). After incubating at 37 °C in a shaker (250 rpm), the culture was used to inoculate 1 L of 2x-YT medium in a 4 L flask, also supplemented with Amp/Cam. The culture was incubated at 37 °C until the OD600 reached ∼0.8, and then, the temperature was lowered to 25 °C for 30 min followed by the addition of 1 mM IPTG to induce protein expression. After overnight incubation, the cells were harvested through centrifugation at 5500 rpm (4 °C), and the resulting cell pellet was stored at −20 °C. After thawing, the cell pellet was resuspended in lysis buffer (0.1 M NaH_2PO_4 buffer pH 7.0 containing 150 mM NaCl, 5 mM imidazole, 5 mM β-mercaptoethanol, and 0.1 mM pyridoxal-5′-phosphate), and the cells were lysed via sonication (6 cycles of 30 s at 18 W with 5 min intervals on ice between cycles). Removal of cell debris was achieved by centrifugation at 40,000 rpm for 1 h, and subsequent purification of TPL was carried out utilizing Ni-NTA chromatography. The column was washed with 0.1 M NaH_2PO_4 buffer at pH 7.0 containing 150 mM NaCl and 5 mM β-mercaptoethanol, supplemented with increasing concentrations of imidazole (0, 5, 10, and 20 mM), after which TPL was eluted using the same buffer containing 250 mM imidazole. Fractions containing TPL were pooled, and imidazole was removed by buffer exchange with 0.1 M NaH_2PO_4 buffer, pH 7.0, containing 150 mM NaCl using ultracentrifuge tubes.

Fluoro-Tyr Synthesis Using Tyrosine Phenol Lyase. Each fluoro-Tyr was synthesized from respective fluorophenol in a reaction mixture comprised of 10 mM fluorophenol, 60 mM pyruvic acid, 40 μM pyridoxal-5′-phosphate, 30 mM ammonium acetate, and 5 mM β-mercaptoethanol that was adjusted to pH 8.0 using NH_4OH.[34,52,53] Subsequently, 160 units/L (0.53 mg = 1 unit) of purified TPL were added followed by incubation in the dark for 4 days at RT. During the incubation, 30 units of TPL were added daily. TPL was then precipitated by acidification of the reaction mixture using 5% trichloroacetic acid and then removed by centrifugation at 5000 rpm (4 °C) and gravity filtration. The supernatant was extracted twice with ethyl acetate to remove excess phenol, and the aqueous layer was then loaded onto an activated cation exchange Amberlite column pre-equilibrated with 200 mL of 2 N HCl and washed with deionized water to eliminate excess HCl. The column was then washed with deionized water, and 250 mL of 10% NH_4OH was used to elute the fluoro-Tyr. Fractions (10 mL) containing fluoro-Tyr were identified using ninhydrin stain (4% ninhydrin), combined, concentrated using a rotary evaporator, and lyophilized. The mass spectra, ^{1}H NMR, and ^{19}F NMR spectra matched that reported previously (see SI).[34]

Fluoro-Tyr Incorporation Using Orthogonal Aminoacyl-tRNA-Synthetases. Unnatural amino acid mutagenesis was performed using engineered aminoacyl-tRNA synthetases.[50,51,54,55] Incorporation of the fluoro-Tyr analogues utilized the E3 orthogonal polyspecific aminoacyl-tRNA synthetase encoded on a pEVOL plasmid[50] and an expression vector for OaPAC with a C-terminal His-tag in which the codon for Y125 had been mutated to TAG. The pCOLD C-terminal His-OaPAC-Y125TAG plasmid (sequence given in the SI) was cotransformed with the E3 pEVOL plasmid into BL21 (AI) cells, and a single colony was utilized to inoculate a 10 mL culture of 2x-YT media, supplemented with 100 μg/mL of ampicillin and 30 μg/mL of chloramphenicol. The culture was incubated overnight at 37 °C on a shaker at 250 rpm, after which 5 mL was used to inoculate 500 mL of 2x-YT media containing 100 μg/mL ampicillin and 30 μg/mL chloramphenicol in a 4 L flask. The culture was incubated at 37 °C in a shaker (250 rpm) until the OD600 reached ∼0.3. Subsequently, 0.05% L-arabinose was added to the medium to induce expression of the E3 aminoacyl-tRNA synthetase. After 1 h, a fluoro-Tyr analogue dissolved in NaOH was added to the media to a final concentration of 1 mM. The OD600 was continuously monitored, and when it reached ∼0.8−1, the temperature was lowered to 18 °C and 1 mM IPTG was added to the media. Following an overnight incubation at 18 °C in a shaker (250 rpm), the cells were harvested via centrifugation at 5500 rpm for 20 min, and the resulting cell pellet was stored at −20 °C prior.

For protein purification, the cell pellet from the 1 L culture was resuspended in 40 mL of lysis buffer (50 mM NaH_2PO_4 pH 8.0, 350 mM NaCl) together with protease inhibitor (PMSF, 250 μM final concentration), β-mercaptoethanol (14 μL), and FAD (10 mg), and the cells were then lysed using sonication. Subsequently, the cell lysate was centrifuged at 40,000 rpm for 1 h at 4 °C to remove cell debris. The supernatant was loaded onto a Ni-NTA column equilibrated with lysis buffer, which was then washed with lysis buffer containing increasing concentrations of imidazole (5, 10, and 20 mM). The OaPAC protein was eluted using lysis buffer containing 250 mM imidazole. Fractions containing OaPAC were pooled, and the imidazole was removed using a HiPrep 26/10 desalting column with 20 mM Tris pH 8.0 buffer containing 150 mM NaCl. After filtering through a 0.22 μm PVDF membrane, the protein purity was confirmed by SDS−PAGE and the concentration was determined by using a UV−visible spectrophotometer. Correct incorporation of the fluoro-Tyr residues was confirmed by mass spectrometry (see the SI).

Incorporation of Azido-Phe (AzPhe). Incorporation of AzPhe was performed using the pDule aminoacyl-tRNA synthetase (pDule-pCNPhe,[51]). The method used followed that described above except that the pCOLD C His-OaPAC-plasmid containing the TAG mutation at the appropriate position was cotransformed with the pDule plasmid and selection was performed using with 100 μg/mL ampicillin and 50 μg/mL spectinomycin. L-arabinose (0.05% w/v) was used to induce the expression of the pDule synthetase, and after 1 h, 110 mg of 4-azido-L-Phe was added as a powder to achieve a final concentration of 1 mM in 2x-YT media. Subsequent purification of the Az-Phe-substituted OaPAC proteins was performed, as described above, and incorporation of the unnatural amino acid was confirmed by mass spectrometry (see SI). In addition, analysis of the tryptic peptides did not reveal any evidence for the presence of amino-Phe (i.e., reduced AzPhe) in the protein. The proteins were concentrated to 2−2.5 mM in 20 mM Tris buffer (pH, 8.0) containing 150 mM

https://doi.org/10.1021/acschembio.4c00627
ACS Chem. Biol. XXXX, XXX, XXX−XXX

NaCl for IR spectroscopy. For experiments in D_2O, the proteins were exchanged into the same buffer prepared using D_2O (pD 8.0).

Steady-State FTIR Spectroscopy. Steady-state FTIR spectra were obtained on a Vertex 80v (Bruker) FTIR spectrometer with a 3 cm^{-1} resolution. The protein sample (50 μL, 2.5 mM in buffer) was placed between two CaF_2 windows with a 6 μm spacer in a Harrick cell, and 256 scans were acquired. The light state was then generated by illuminating the sample continuously using a 455 nm LED (Prizmatix, Ltd.) placed into the sample compartment and focused onto the cell. The dark state spectrum was subtracted from the light state spectrum to generate the light minus dark (L-D) difference spectrum. The dark and light steady state spectra were obtained by subtracting the spectrum of the buffer measured with the same parameters as protein samples. All measurements were performed at RT. We used 450 nm LED to irradiate the samples, and the spectrum of AzPhe before irradiation and after several rounds of irradiation was compared to ensure that there was no photodegradation of the azido on blue light irradiation (Figure S4).

Time-Resolved Multiple Probe Spectroscopy (TRMPS). TRMPS spectra were obtained at 20 °C from 100 fs to 1 ms at the STFC Central Laser Facility. The TRMPS method has been described and previously used by us to analyze the photochemistry and site-specific protein dynamics of BLUF proteins.[34,56,57] Light sensitive samples were analyzed using a rastered flow cell to minimize photochemistry, and data were acquired using a 450 nm pump operated at 0.6−0.8 μJ per pulse and a repetition rate of 1 kHz. The spectral resolution was 3 cm^{-1}, and the temporal resolution was 200 fs. For the AzPhe measurement in the region of 2050−2200 cm^{-1}, the W90AzPhe protein was concentrated to ∼2 mM in H_2O buffer (20 mM Tris, 150 mM NaCl, pH 8.0). For the fingerprint region, the sample was buffer exchanged to D_2O buffer (20 mM Tris, 150 mM NaCl, pD 8.0) and concentrated to ∼0.8 mM. After the measurements were recorded, the extent of photoconversion was shown to be negligible using absorbance spectroscopy. Spectra were calibrated relative to the IR transmission of a pure *cis* stilbene standard sample placed at the sample position. Data were analyzed globally using the sequential model with Glotaran.

Adenylate Cyclase Activity Assay. The adenylate cyclase activity of the aqueous phase of OaPAC was performed using an Ocean Optics spectrophotometer equipped with a 12.5 mm width, 10 mm path length quartz cuvette. Assays contained OaPAC (1 μM), ATP (10−800 μM), and the master mix of reagents which contained inorganic pyrophosphatase, purine nucleoside phosphorylase, 20X buffer (1 M Tris−HCl, 20 mM $MgCl_2$, pH 7.5), and dH_2O as diluent. In this coupled assay, the PPi produced from the conversion of ATP to cAMP is converted to two equiv of Pi by inorganic pyrophosphatase, and the Pi is then quantified following reaction with MESG/PNP and detection at 360 nm. The reaction mixture was incubated in the cuvette in the dark, and absorbance at 360 nm was monitored for 40 s. The cuvette was then continuously illuminated with blue light, and absorbance was monitored at 360 nm to determine initial velocities.

■ ASSOCIATED CONTENT

Supporting Information

The Supporting Information is available free of charge at https://pubs.acs.org/doi/10.1021/acschembio.4c00627.

Dark and light state absorbance spectra, recovery kinetics, and Michaelis−Menten plots (PDF)

■ AUTHOR INFORMATION

Corresponding Authors

Andras Lukacs − *Department of Biophysics, Medical School, University of Pecs, 7624 Pecs, Hungary;* orcid.org/0000-0001-8841-9823; Email: andras.lukacs@aok.pte.hu

Stephen R. Meech − *School of Chemistry, University of East Anglia, Norwich NR4 7TJ, U.K.;* orcid.org/0000-0001-5561-2782; Email: s.meech@uea.ac.uk

Peter J. Tonge − *Department of Chemistry, Stony Brook University, Stony Brook, New York 11794-3400, United States; School of Chemistry, University of East Anglia, Norwich NR4 7TJ, U.K.;* orcid.org/0000-0003-1606-3471; Email: peter.tonge@stonybrook.edu

Authors

Samruddhi S. Jewlikar − *Department of Chemistry, Stony Brook University, Stony Brook, New York 11794-3400, United States*

Jinnette Tolentino Collado − *Chemistry Department, Farmingdale State College, Farmingdale, New York 11735, United States*

Madeeha I. Ali − *Department of Chemistry, Stony Brook University, Stony Brook, New York 11794-3400, United States;* orcid.org/0009-0005-9329-3475

Aya Sabbah − *Department of Chemistry, Stony Brook University, Stony Brook, New York 11794-3400, United States*

YongLe He − *Department of Chemistry, Stony Brook University, Stony Brook, New York 11794-3400, United States*

James N. Iuliano − *Department of Chemistry, Stony Brook University, Stony Brook, New York 11794-3400, United States;* orcid.org/0000-0003-1213-3292

Christopher R. Hall − *School of Chemistry, University of East Anglia, Norwich NR4 7TJ, U.K.;* Present Address: Present address: ARC Centre of Excellence in Exciton Science, School of Chemistry, The University of Melbourne, Parkville, Victoria 3010, Australia

Katrin Adamczyk − *School of Chemistry, University of East Anglia, Norwich NR4 7TJ, U.K.*

Gregory M. Greetham − *Central Laser Facility, Research Complex at Harwell, Rutherford Appleton Laboratory, Didcot OX11 0QX, U.K.;* orcid.org/0000-0002-1852-3403

Complete contact information is available at: https://pubs.acs.org/10.1021/acschembio.4c00627

Notes

The authors declare no competing financial interest.

■ ACKNOWLEDGMENTS

This study was supported by the National Science Foundation (NSF) (MCB-1817837 to PJT) and the EPSRC (EP/N033647/1 to S.R.M.). A.L. acknowledges funding from the Hungarian National Research and Innovation Office (K-137557) and was supported by PTE ÁOK-KA-2021. J.T.C. and A.S were supported by the NY-CAPs IRACDA (K12-GM102778) Program at Stony Brook University. Y.H., J.N.I and M.I.A. were supported by a National Institutes of Health Chemistry-Biology Interface Training Grant (T32GM092714; T32GM136572). The authors are grateful to STFC for access to the ULTRA laser facility.

■ ABBREVIATIONS

BLUF, blue light utilizing flavin; FAD, flavin adenine dinucleotide; TRMPS, time-resolved multiple probe spectroscopy; TRIR, time-resolved infrared spectroscopy; EADS, evolution associated difference spectra

REFERENCES

(1) Deisseroth, K. Optogenetics. *Nat. Methods* **2011**, *8*, 26−29.
(2) Moglich, A.; Moffat, K. Engineered photoreceptors as novel optogenetic tools. *Photochem. Photobiol. Sci.* **2010**, *9*, 1286−1300.
(3) Lindner, F.; Diepold, A. Optogenetics in bacteria—applications and opportunities. *FEMS Microbiol. Rev.* **2022**, *46*, No. fuab055.
(4) Iuliano, J. N.; Collado, J. T.; Gil, A. A.; Ravindran, P. T.; Lukacs, A.; Shin, S.; Woroniecka, H. A.; Adamczyk, K.; Aramini, J. M.; Edupuganti, U. R.; Hall, C. R.; Greetham, G. M.; Sazanovich, I. V.; Clark, I. P.; Daryaee, T.; Toettcher, J. E.; French, J. B.; Gardner, K. H.; Simmerling, C. L.; Meech, S. R.; Tonge, P. J. Unraveling the Mechanism of a LOV Domain Optogenetic Sensor: A Glutamine Lever Induces Unfolding of the Jalpha Helix. *ACS Chem. Biol.* **2020**, *15*, 2752−2765.
(5) Lukacs, A.; Tonge, P. J.; Meech, S. R. Photophysics of the Blue Light Using Flavin Domain. *Acc. Chem. Res.* **2022**, *55*, 402−414.
(6) Gomelsky, M.; Klug, G. BLUF: a novel FAD-binding domain involved in sensory transduction in microorganisms. *Trends Biochem. Sci.* **2002**, *27*, 497−500.
(7) Masuda, S.; Bauer, C. E. AppA is a blue light photoreceptor that antirepresses photosynthesis gene expression in Rhodobacter sphaeroides. *Cell* **2002**, *110*, 613−623.
(8) Okajima, K.; Yoshihara, S.; Fukushima, Y.; Geng, X.; Katayama, M.; Higashi, S.; Watanabe, M.; Sato, S.; Tabata, S.; Shibata, Y.; Itoh, S.; Ikeuchi, M. Biochemical and functional characterization of BLUF-type flavin-binding proteins of two species of cyanobacteria. *J. Biochem* **2005**, *137*, 741−750.
(9) Tuttobene, M. R.; Cribb, P.; Mussi, M. A. BlsA integrates light and temperature signals into iron metabolism through Fur in the human pathogen Acinetobacter baumannii. *Sci. Rep* **2018**, *8*, 7728.
(10) Iseki, M.; Matsunaga, S.; Murakami, A.; Ohno, K.; Shiga, K.; Yoshida, K.; Sugai, M.; Takahashi, T.; Hori, T.; Watanabe, M. A blue-light-activated adenylyl cyclase mediates photoavoidance in Euglena gracilis. *Nature* **2002**, *415*, 1047−1051.
(11) Stierl, M.; Stumpf, P.; Udwari, D.; Gueta, R.; Hagedorn, R.; Losi, A.; Gartner, W.; Petereit, L.; Efetova, M.; Schwarzel, M.; Oertner, T. G.; Nagel, G.; Hegemann, P. Light modulation of cellular cAMP by a small bacterial photoactivated adenylyl cyclase, bPAC, of the soil bacterium Beggiatoa. *J. Biol. Chem.* **2011**, *286*, 1181−1188.
(12) Ohki, M.; Sugiyama, K.; Kawai, F.; Tanaka, H.; Nihei, Y.; Unzai, S.; Takebe, M.; Matsunaga, S.; Adachi, S.; Shibayama, N.; Zhou, Z.; Koyama, R.; Ikegaya, Y.; Takahashi, T.; Tame, J. R.; Iseki, M.; Park, S. Y. Structural insight into photoactivation of an adenylate cyclase from a photosynthetic cyanobacterium. *Proc. Natl. Acad. Sci. U. S. A.* **2016**, *113*, 6659−6664.
(13) Anderson, S.; Dragnea, V.; Masuda, S.; Ybe, J.; Moffat, K.; Bauer, C. Structure of a novel photoreceptor, the BLUF domain of AppA from Rhodobacter sphaeroides. *Biochemistry* **2005**, *44*, 7998−8005.
(14) Jung, A.; Domratcheva, T.; Tarutina, M.; Wu, Q.; Ko, W. H.; Shoeman, R. L.; Gomelsky, M.; Gardner, K. H.; Schlichting, I. Structure of a bacterial BLUF photoreceptor: insights into blue light-mediated signal transduction. *Proc. Natl. Acad. Sci. U. S. A.* **2005**, *102*, 12350−12355.
(15) Grinstead, J. S.; Hsu, S. T.; Laan, W.; Bonvin, A. M.; Hellingwerf, K. J.; Boelens, R.; Kaptein, R. The solution structure of the AppA BLUF domain: insight into the mechanism of light-induced signaling. *Chembiochem* **2006**, *7*, 187−193.
(16) Jung, A.; Reinstein, J.; Domratcheva, T.; Shoeman, R. L.; Schlichting, I. Crystal structures of the AppA BLUF domain photoreceptor provide insights into blue light-mediated signal transduction. *J. Mol. Biol.* **2006**, *362*, 717−732.
(17) Masuda, S.; Hasegawa, K.; Ishii, A.; Ono, T. A. Light-induced structural changes in a putative blue-light receptor with a novel FAD binding fold sensor of blue-light using FAD (BLUF); Slr1694 of synechocystis sp. PCC6803. *Biochemistry* **2004**, *43*, 5304−5313.
(18) Unno, M.; Masuda, S.; Ono, T. A.; Yamauchi, S. Orientation of a key glutamine residue in the BLUF domain from AppA revealed by mutagenesis, spectroscopy, and quantum chemical calculations. *J. Am. Chem. Soc.* **2006**, *128*, 5638−5639.
(19) Stelling, A. L.; Ronayne, K. L.; Nappa, J.; Tonge, P. J.; Meech, S. R. Ultrafast structural dynamics in BLUF domains: transient infrared spectroscopy of AppA and its mutants. *J. Am. Chem. Soc.* **2007**, *129*, 15556−15564.
(20) Domratcheva, T.; Grigorenko, B. L.; Schlichting, I.; Nemukhin, A. V. Molecular models predict light-induced glutamine tautomerization in BLUF photoreceptors. *Biophys. J.* **2008**, *94*, 3872−3879.
(21) Udvarhelyi, A.; Domratcheva, T. Photoreaction in BLUF Receptors: Proton-coupled Electron Transfer in the Flavin-Gln-Tyr System. *Photochem. Photobiol.* **2011**, *87*, 554−563.
(22) Domratcheva, T.; Hartmann, E.; Schlichting, I.; Kottke, T. Evidence for Tautomerisation of Glutamine in BLUF Blue Light Receptors by Vibrational Spectroscopy and Computational Chemistry. *Sci. Rep* **2016**, *6*, 22669.
(23) Iwata, T.; Nagai, T.; Ito, S.; Osoegawa, S.; Iseki, M.; Watanabe, M.; Unno, M.; Kitagawa, S.; Kandori, H. Hydrogen Bonding Environments in the Photocycle Process around the Flavin Chromophore of the AppA-BLUF domain. *J. Am. Chem. Soc.* **2018**, *140*, 11982−11991.
(24) Goings, J. J.; Li, P.; Zhu, Q.; Hammes-Schiffer, S. Formation of an unusual glutamine tautomer in a blue light using flavin photocycle characterizes the light-adapted state. *Proc. Natl. Acad. Sci. U. S. A.* **2020**, *117*, 26626−26632.
(25) Hontani, Y.; Mehlhorn, J.; Domratcheva, T.; Beck, S.; Kloz, M.; Hegemann, P.; Mathes, T.; Kennis, J. T. M. Spectroscopic and Computational Observation of Glutamine Tautomerization in the Blue Light Sensing Using Flavin Domain Photoreaction. *J. Am. Chem. Soc.* **2023**, *145*, 1040−1052.
(26) Chretien, A.; Nagel, M. F.; Botha, S.; de Wijn, R.; Brings, L.; Dorner, K.; Han, H.; Koliyadu, J. C. P.; Letrun, R.; Round, A.; Sato, T.; Schmidt, C.; Secareanu, R. C.; von Stetten, D.; Vakili, M.; Wrona, A.; Bean, R.; Mancuso, A.; Schulz, J.; Pearson, A. R.; Kottke, T.; Lorenzen, K.; Schubert, R. Light-induced Trp(in)/Met(out) Switching During BLUF Domain Activation in ATP-bound Photoactivatable Adenylate Cyclase OaPAC. *J. Mol. Biol.* **2024**, *436*, No. 168439.
(27) PyMOL. The PyMOL Molecular Graphics System, Version 2.5 Schrödinger, LLC, 2015.
(28) Lukacs, A.; Haigney, A.; Brust, R.; Zhao, R. K.; Stelling, A. L.; Clark, I. P.; Towrie, M.; Greetham, G. M.; Meech, S. R.; Tonge, P. J. Photoexcitation of the blue light using FAD photoreceptor AppA results in ultrafast changes to the protein matrix. *J. Am. Chem. Soc.* **2011**, *133*, 16893−16900.
(29) Unno, M.; Kikuchi, S.; Masuda, S. Structural refinement of a key tryptophan residue in the BLUF photoreceptor AppA by ultraviolet resonance Raman spectroscopy. *Biophys. J.* **2010**, *98*, 1949−1956.
(30) Pandey, R.; Flockerzi, D.; Hauser, M. J.; Straube, R. Modeling the light- and redox-dependent interaction of PpsR/AppA in Rhodobacter sphaeroides. *Biophys. J.* **2011**, *100*, 2347−2355.
(31) Dragnea, V.; Arunkumar, A. I.; Lee, C. W.; Giedroc, D. P.; Bauer, C. E. A Q63E Rhodobacter sphaeroides AppA BLUF domain mutant is locked in a pseudo-light-excited signaling state. *Biochemistry* **2010**, *49*, 10682−10690.
(32) Gil, A. A.; Haigney, A.; Laptenok, S. P.; Brust, R.; Lukacs, A.; Iuliano, J. N.; Jeng, J.; Melief, E. H.; Zhao, R. K.; Yoon, E.; Clark, I. P.; Towrie, M.; Greetham, G. M.; Ng, A.; Truglio, J. J.; French, J. B.; Meech, S. R.; Tonge, P. J. Mechanism of the AppABLUF Photocycle Probed by Site-Specific Incorporation of Fluorotyrosine Residues: Effect of the Y21 pKa on the Forward and Reverse Ground-State Reactions. *J. Am. Chem. Soc.* **2016**, *138*, 926−935.
(33) Lukacs, A.; Brust, R.; Haigney, A.; Laptenok, S. P.; Addison, K.; Gil, A.; Towrie, M.; Greetham, G. M.; Tonge, P. J.; Meech, S. R. BLUF domain function does not require a metastable radical intermediate state. *J. Am. Chem. Soc.* **2014**, *136*, 4605−4615.
(34) Tolentino Collado, J.; Iuliano, J. N.; Pirisi, K.; Jewlikar, S.; Adamczyk, K.; Greetham, G. M.; Towrie, M.; Tame, J. R. H.; Meech, S. R.; Tonge, P. J.; Lukacs, A. Unraveling the Photoactivation

https://doi.org/10.1021/acschembio.4c00627
ACS Chem. Biol. XXXX, XXX, XXX−XXX

Mechanism of a Light-Activated Adenylyl Cyclase Using Ultrafast Spectroscopy Coupled with Unnatural Amino Acid Mutagenesis. *ACS Chem. Biol.* **2022**, *17*, 2643−2654.
(35) Tolentino Collado, J.; Bodis, E.; Pasitka, J.; Szucs, M.; Fekete, Z.; Kis-Bicskei, N.; Telek, E.; Pozsonyi, K.; Kapetanaki, S. M.; Greetham, G.; Tonge, P. J.; Meech, S. R.; Lukacs, A. Single Amino Acid Mutation Decouples Photochemistry of the BLUF Domain from the Enzymatic Function of OaPAC and Drives the Enzyme to a Switched-on State. *J. Mol. Biol.* **2024**, *436*, No. 168312.
(36) Raics, K.; Pirisi, K.; Zhuang, B.; Fekete, Z.; Kis-Bicskei, N.; Pecsi, I.; Ujfalusi, K. P.; Telek, E.; Li, Y.; Collado, J. T.; Tonge, P. J.; Meech, S. R.; Vos, M. H.; Bodis, E.; Lukacs, A. Photocycle alteration and increased enzymatic activity in genetically modified photoactivated adenylate cyclase OaPAC. *J. Biol. Chem.* **2023**, *299*, No. 105056.
(37) Ohki, M.; Sato-Tomita, A.; Matsunaga, S.; Iseki, M.; Tame, J. R. H.; Shibayama, N.; Park, S. Y. Molecular mechanism of photoactivation of a light-regulated adenylate cyclase. *Proc. Natl. Acad. Sci. U. S. A.* **2017**, *114*, 8562−8567.
(38) Hall, C. R.; Tolentino Collado, J.; Iuliano, J. N.; Gil, A. A.; Adamczyk, K.; Lukacs, A.; Greetham, G. M.; Sazanovich, I.; Tonge, P. J.; Meech, S. R. Site-Specific Protein Dynamics Probed by Ultrafast Infrared Spectroscopy of a Noncanonical Amino Acid. *J. Phys. Chem. B* **2019**, *123*, 9592−9597.
(39) Krause, B. S.; Kaufmann, J. C. D.; Kuhne, J.; Vierock, J.; Huber, T.; Sakmar, T. P.; Gerwert, K.; Bartl, F. J.; Hegemann, P. Tracking Pore Hydration in Channelrhodopsin by Site-Directed Infrared-Active Azido Probes. *Biochemistry* **2019**, *58*, 1275−1286.
(40) Kurttila, M.; Stucki-Buchli, B.; Rumfeldt, J.; Schroeder, L.; Hakkanen, H.; Liukkonen, A.; Takala, H.; Kottke, T.; Ihalainen, J. A. Site-by-site tracking of signal transduction in an azidophenylalanine-labeled bacteriophytochrome with step-scan FTIR spectroscopy. *Phys. Chem. Chem. Phys.* **2021**, *23*, 5615−5628.
(41) Noren, C. J.; Anthony-Cahill, S. J.; Griffith, M. C.; Schultz, P. G. A general method for site-specific incorporation of unnatural amino acids into proteins. *Science* **1989**, *244*, 182−188.
(42) Lindner, R.; Hartmann, E.; Tarnawski, M.; Winkler, A.; Frey, D.; Reinstein, J.; Meinhart, A.; Schlichting, I. Photoactivation Mechanism of a Bacterial Light-Regulated Adenylyl Cyclase. *J. Mol. Biol.* **2017**, *429*, 1336−1351.
(43) Yuan, H.; Anderson, S.; Masuda, S.; Dragnea, V.; Moffat, K.; Bauer, C. Crystal structures of the Synechocystis photoreceptor Slr1694 reveal distinct structural states related to signaling. *Biochemistry* **2006**, *45*, 12687−12694.
(44) Masuda, S.; Tomida, Y.; Ohta, H.; Takamiya, K. The critical role of a hydrogen bond between Gln63 and Trp104 in the blue-light sensing BLUF domain that controls AppA activity. *J. Mol. Biol.* **2007**, *368*, 1223−1230.
(45) Brust, R.; Lukacs, A.; Haigney, A.; Addison, K.; Gil, A.; Towrie, M.; Clark, I. P.; Greetham, G. M.; Tonge, P. J.; Meech, S. R. Proteins in action: femtosecond to millisecond structural dynamics of a photoactive flavoprotein. *J. Am. Chem. Soc.* **2013**, *135*, 16168−16174.
(46) Tokonami, S.; Onose, M.; Nakasone, Y.; Terazima, M. Slow Conformational Changes of Blue Light Sensor BLUF Proteins in Milliseconds. *J. Am. Chem. Soc.* **2022**, *144*, 4080−4090.
(47) Goyal, P.; Hammes-Schiffer, S. Role of active site conformational changes in photocycle activation of the AppA BLUF photoreceptor. *Proc. Natl. Acad. Sci. U. S. A.* **2017**, *114*, 1480−1485.
(48) Zhou, Y.; Tang, S.; Chen, Z.; Zhou, Z.; Huang, J.; Kang, X. W.; Zou, S.; Wang, B.; Zhang, T.; Ding, B.; Zhong, D. Origin of the multiphasic quenching dynamics in the BLUF domains across the species. *Nat. Commun.* **2024**, *15*, 623.
(49) Nakasone, Y.; Murakami, H.; Tokonami, S.; Oda, T.; Terazima, M. Time-resolved study on signaling pathway of photoactivated adenylate cyclase and its nonlinear optical response. *J. Biol. Chem.* **2023**, *299*, No. 105285.
(50) Minnihan, E. C.; Young, D. D.; Schultz, P. G.; Stubbe, J. Incorporation of Fluorotyrosines into Ribonucleotide Reductase Using an Evolved, Polyspecific Aminoacyl-tRNA Synthetase. *J. Am. Chem. Soc.* **2011**, *133*, 15942−15945.
(51) Miyake-Stoner, S. J.; Miller, A. M.; Hammill, J. T.; Peeler, J. C.; Hess, K. R.; Mehl, R. A.; Brewer, S. H. Probing protein folding using site-specifically encoded unnatural amino acids as FRET donors with tryptophan. *Biochemistry* **2009**, *48*, 5953−5962.
(52) Seyedsayamdost, M. R.; Yee, C. S.; Stubbe, J. Site-specific incorporation of fluorotyrosines into the R2 subunit of E. coli ribonucleotide reductase by expressed protein ligation. *Nat. Protoc* **2007**, *2*, 1225−1235.
(53) Seyedsayamdost, M. R.; Reece, S. Y.; Nocera, D. G.; Stubbe, J. Mono-, di-, tri-, and tetra-substituted fluorotyrosines: new probes for enzymes that use tyrosyl radicals in catalysis. *J. Am. Chem. Soc.* **2006**, *128*, 1569−1579.
(54) Young, D. D.; Schultz, P. G. Playing with the Molecules of Life. *ACS Chem. Biol.* **2018**, *13*, 854−870.
(55) de la Torre, D.; Chin, J. W. Reprogramming the genetic code. *Nat. Rev. Genet* **2021**, *22*, 169−184.
(56) Greetham, G. M.; Sole, D.; Clark, I. P.; Parker, A. W.; Pollard, M. R.; Towrie, M. Time-resolved multiple probe spectroscopy. *Rev. Sci. Instrum.* **2012**, *83*, 103107.
(57) Greetham, G. M.; Burgos, P.; Cao, Q.; Clark, I. P.; Codd, P. S.; Farrow, R. C.; George, M. W.; Kogimtzis, M.; Matousek, P.; Parker, A. W.; Pollard, M. R.; Robinson, D. A.; Xin, Z. J.; Towrie, M. ULTRA: A Unique Instrument for Time-Resolved Spectroscopy. *Appl. Spectrosc.* **2010**, *64*, 1311−1319.

https://doi.org/10.1021/acschembio.4c00627
ACS Chem. Biol. XXXX, XXX, XXX−XXX